AIP | Applied Physics Letters

Alumina nanoparticle/polymer nanocomposite dielectric for flexible amorphous indium-gallium-zinc oxide thin film transistors on plastic substrate with superior stability

Hsin-Cheng Lai, Zingway Pei, Jyun-Ruri Jian, and Bo-Jie Tzeng

Citation: Applied Physics Letters **105**, 033510 (2014); doi: 10.1063/1.4891426
View online: http://dx.doi.org/10.1063/1.4891426
View Table of Contents: http://scitation.aip.org/content/aip/journal/apl/105/3?ver=pdfcov
Published by the AIP Publishing

Alumina nanoparticle/polymer nanocomposite dielectric for flexible amorphous indium-gallium-zinc oxide thin film transistors on plastic substrate with superior stability

Hsin-Cheng Lai,[1] Zingway Pei,[1,2,3,a)] Jyun-Ruri Jian,[2] and Bo-Jie Tzeng[2]
[1]*Department of Electrical Engineering, National Chung Hsing University, Taichung 40227, Taiwan*
[2]*Graduate Institute of Optoelectronic Engineering, National Chung Hsing University, Taichung 40227, Taiwan*
[3]*Center of Nanoscience and Nanotechnology, National Chung Hsing University, Taichung 40227, Taiwan*

(Received 5 June 2014; accepted 13 July 2014; published online 24 July 2014)

In this study, the Al_2O_3 nanoparticles were incorporated into polymer as a nono-composite dielectric for used in a flexible amorphous Indium-Gallium-Zinc Oxide (a-IGZO) thin-film transistor (TFT) on a polyethylene naphthalate substrate by solution process. The process temperature was well below 100 °C. The a-IGZO TFT exhibit a mobility of 5.13 cm^2/V s on the flexible substrate. After bending at a radius of 4 mm (strain = 1.56%) for more than 100 times, the performance of this a-IGZO TFT was nearly unchanged. In addition, the electrical characteristics are less altered after positive gate bias stress at 10 V for 1500 s. Thus, this technology is suitable for use in flexible displays. © *2014 AIP Publishing LLC*. [http://dx.doi.org/10.1063/1.4891426]

Amorphous indium-gallium-zinc oxide thin film transistors (a-IGZO TFTs) have been extensively investigated in recent years.[1,2] Compared with other materials, a-IGZO TFTs yield high mobility, exhibit uniform material structures, and are compatible with contemporary large area manufacturing processes; thus, these TFTs are suitable for flexible displays on light-weight plastic substrates. For TFT on flexible substrate, the mobility as high as 24.26 cm^2/V s, with 9 orders of magnitude current on-off ratio has been demonstrated on PEN substrate utilize inorganic gate dielectric (AlO_x).[3] The flexible a-IGZO TFT organic light-emitting diode (OLED) display has also been demonstrated on PEN substrate.[4] To achieve both high performance and high flexibility, a-IGZO TFTs are typically fabricated at high temperatures on plastic substrates having high glass transition temperature (T_g), such as polyimide, at substrate thicknesses less than 50 μm.[5,7] Thin substrates enable a-IGZO TFTs to be bent at a radius less than 5 mm, yielding a highest strain more than 1%.[6] However, real displays do not only comprise substrate; for example, the encapsulation layer and display material such as OLEDs must be included. After adding OLEDs and encapsulation layers, high strain levels could possible limit the flexibility.[8] An a-IGZO TFT comprising a polymer gate dielectric was suggested as alternative method than inorganic dielectric for TFTs to sustain high strain.[9] The Young's modulus for polymer material is around 1 GPa, whereas it is higher than 100 GPa for oxide-based inorganic semiconductors. This large difference cause the deformation of materials that occurs at high strain levels primarily on the polymer, leaving the properties of the a-IGZO layer less altered after bending at high strain (1.5%). Although a-IGZO TFTs that comprise polymer dielectrics can be bent at high strain levels without degrading the performance, the polymer is a soft material; thus, the plasma involved in a-IGZO deposition may damage polymer, either inside the film or on the surfaces, causing low mobility. Recently, the high dielectric constant nanoparticle (NP) incorporated polymer, named nanocomposite polymer, was demonstrated to have good flexibility as a gate dielectric for organic TFTs.[10] However, the robustness of this nanocomposite dielectric was not studied by stress under high electrical field. In this study, AlO_x NPs were incorporated in a polymer as a nanocomposite gate dielectric for an a-IGZO TFT. The performance of this a-IGZO TFT was evaluated by the current-voltage characteristics, bending test and positive-bias stress test.

Figure 1(a) shows a schematic diagram of the a-IGZO TFT on a 125–μm-thick polyethylene naphthalate (PEN) substrate, using a polymer nanocomposite as a gate dielectric. A 400-nm-thick cross-linked polymer layer was coated on the PEN as a smoothing layer prior to fabricating the

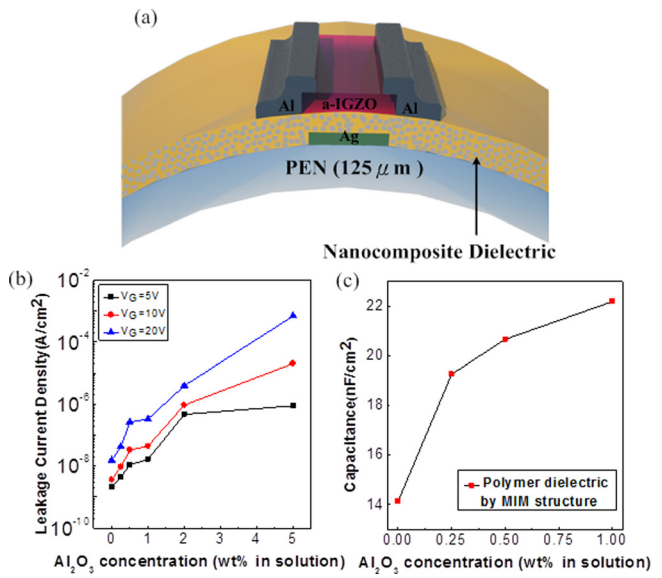

FIG. 1. (a) The schematic diagram of the flexible a-IGZO TFT on PEN substrate and (b) leakage current density of nanocomposite layer. (c) Capacitance of nanocomposite layer.

a)Electronic mail: zingway@dragon.nchu.edu.tw

TFT. Silver (Ag) gate material was deposited on the PEN through a pre-patterned metal foil (shadow mask) by thermal evaporation in 50-nm-thick. The polymer solution consisting of poly (4-vinylphenol) (PVP) and poly (melamine-co-formaldehyde) (PMF) at a ratio of 2:1 dissolved in n-butanol was used for gate dielectric. This polymer was also used as a smoothing layer. Regarding the nanocomposite polymer, aluminum oxide (Al_2O_3) NPs were added to the PVP/PMF precursor at a concentration from 0.25 to 1.0 wt. % in solution. The Al_2O_3 NPs (sizes < 50 nm) were purchased from Sigma-Aldrich. To prepare the 0.25 wt. % precursor, 2 g of PVP and 1 g of PMF were first dissolved in the 40 g of n-butanol. Then 5 g of solution was drawing out. The 12.5 mg of Al_2O_3 was add into this solution to form 0.25 wt. % precursor. After being stirred overnight, the solution was spin-coated onto the silver gate at 1000 rpm for 60 s. The polymer layer was subsequently dried on a hot plate at 100 °C for 10 min and cross-linked in a nitrogen environment by using ultraviolet (254 nm) light illumination for 60 min. The thickness of the nanocomposite polymer ($Al_2O_3 = 0.25$ wt. %) was approximately 286.9 nm as determined using scanning electron microscopy. In contrast, the thickness of polymer without Al_2O_3 NPs is 249.4 nm. After fabricating nanocomposite gate dielectric, a 60-nm-thick a-IGZO layer was deposited through a shadow mask by using radio frequency (RF, 13.56 MHz) magnetron sputtering at room temperature in an Ar environment. The RF power was 20 W and the working pressure was 5 mTorr. The InGaZnO4 (1:1:1:4) target was purchased from Mitsui Co. Finally, Aluminum (Al) was used to fabricate the source/drain electrode. The source/drain was deposited at a thickness of 40 nm by using an associated shadow mask by a thermal evaporator. The channel length (L) and channel width (W) of the fabricated a-IGZO TFTs were 100 μm and 500 μm, respectively. The device characteristics of the a-IGZO TFTs were measured using an Agilent 2912A semiconductor parameter analyzer in a dark environment on a probe station.

To measure the leakage current and capacitance of the nanocomposite polymer, a metal-insulator-metal structure was fabricated using 100-nm-thick Al metal. Fig. 1(b) displays the leakage current density for the nanocomposite dielectrics at various Al_2O_3 concentrations. The pure PVP polymer gate dielectric yielded the lowest leakage current density of approximately 3×10^{-9} A/cm^2 at 10 V. The leakage current density increased as the concentration of Al_2O_3 increased, and extensively leaked after reaching 1 wt. % of Al_2O_3 (4.4×10^{-8} A/cm^2). The leakage current densities for the polymer nanocomposite at 0.25 and 0.5 wt. % Al_2O_3 were 9×10^{-9} and 3×10^{-8} A/cm^2, respectively, at 10 V. The leakage current density of 0.25 wt. % of Al_2O_3 is in the same order of magnitude to pure PVP polymers; thus, polymer nanocomposites with low Al_2O_3 concentration are likely suitable for application in TFTs. Fig. 1(c) shows the capacitance density for nanocomposite dielectric regarding various Al_2O_3 concentrations. The capacitance density of the pure PVP was 14 nF/cm^2. The dielectric constant was calculated as 3.9. After adding 0.25 wt. % Al_2O_3, the capacitance density increased to 19 nF/cm^2; the corresponding dielectric constant is 6.1. Further increasing the percentage of Al_2O_3 nanoparticles in the solution to 0.5 and 1.0 wt. % increased the capacitance density to 20 and 22 nF/cm^2, respectively, yielding corresponding dielectric constants of 7.1 and 8.1, respectively. This capacitance and leakage current investigation suggested that a 0.25 wt. % concentration of Al_2O_3 NPs is suitable for application in TFTs. Take the dielectric constant of Al_2O_3 NPs is 9–11 into account, the 6.1 dielectric constant for nanocomposite layer indicates the solid content of Al_2O_3 NPs ranged from 43% to 31%. The cross-sectional scanning electron microscopy image of cross-linked PVP polymer and PVP/Al_2O_3 NPs polymer dielectric were shown in Figs. 2(a) and 2(b), respectively. Both surfaces are smooth according to SEM images. In Fig. 2(b), the aggregation of Al_2O_3 NPs was not found. Since the interface of a-IGZO/dielectric is very important to the current-voltage characteristics of a TFT, the surface topography was explored by atomic force microscopy (AFM). The AFM images were depicted in Figs. 2(c) and 2(d) for PVP polymer and PVP/Al_2O_3 NPs nanocomposite layer, respectively. The PVP surface is extremely smooth. A root-mean-square (RMS) roughness of 0.274 nm was obtained. In contrast, the nanocomposite layer is not so smooth. The RMS roughness is 3.51 nm. Some protrusions were found. However, the protrusion covers very small area. This indicates the aggregations of Al_2O_3 NPs in some area. This is reasonable since the solid content of Al_2O_3 NPs probably as high as 43%. Such a small-area protrusion may not affect the TFT characteristics since the current could flow around this region. This argument could be clarified by the current-voltage characteristics of a-IGZO TFT. Figure 3 depicts the transfer characteristics (I_D-V_G) of the a-IGZO TFT fabricated on a PEN substrate. Figure 3(a) depicts the I_D-V_G for a-IGZO TFT with PVP as gate dielectric. The drain current is approximately 1 μA at gate-to-source voltage of 10 V. The mobility (μ), subthreshold swing (S.S.), drain current on/off ratio (I_{on}/I_{off}), and threshold voltage (V_{th}) of this a-IGZO TFT are 0.8 cm^2/V s, 1.1 V/dec., 1.3×10^4, and -1.4 V, respectively, as listed in Table I. After incorporating the Al_2O_3 NPs, The drain current enhanced 5 times to approximately 5 μA as shown in

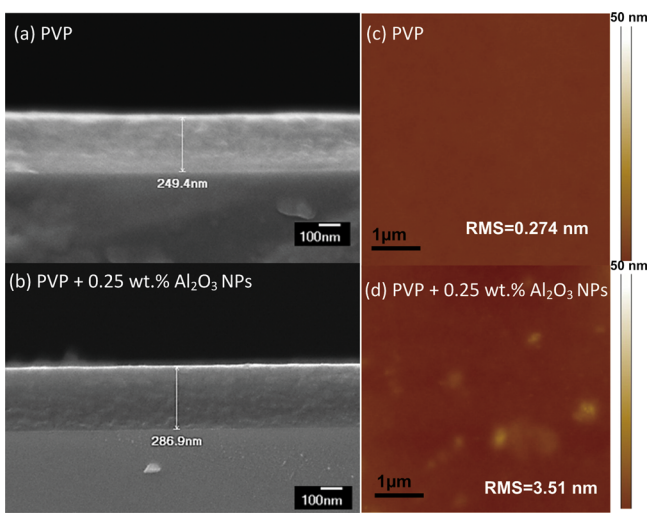

FIG. 2. The cross-sectional scanning electron microscopy images of (a) PVP dielectric, (b) PVP/Al_2O_3 NPs nanocomposite gate dielectric and the surface topography by atomic force microscopy for (c) PVP dielectric, (d) PVP/Al_2O_3 NPs nanocomposite gate dielectric.

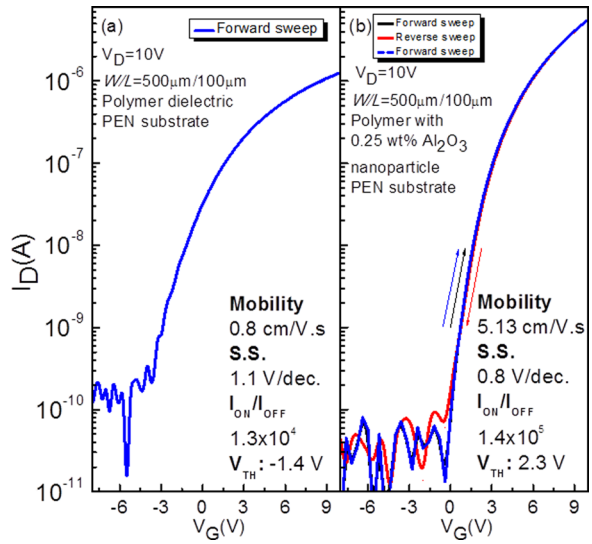

FIG. 3. Transfer characteristics of a-IGZO TFT on PEN substrate with (a) PVP gate dielectric and (b) PVP/Al_2O_3 NPs nanocomposite gate dielectric.

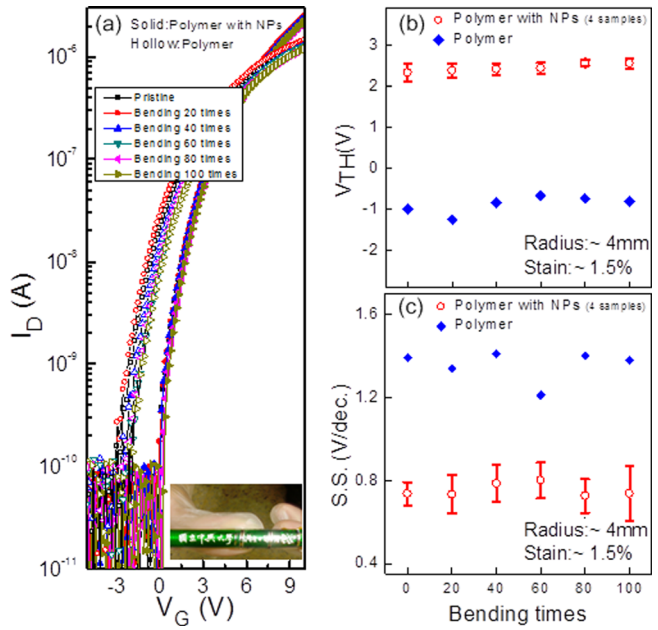

FIG. 4. (a) Transfer characteristics, (b) the threshold (V_{th}), and (c) the sub-threshold swing (S.S) for a-IGZO TFT nanocomposite gate dielectric after bending (radius: 4 mm) for 100 times. The V_{TH} and S.S. are counted for 4 samples.

Fig. 3(b). The gate voltage was swept forward and reverses between −10 V and 10 V for three times. No hysteresis was found. The threshold voltage was shifted positively from −1.4 to 2.3 V, indicates the a-IGZO TFT operates from depletion mode to enhancement mode TFT operation. The mobility increased to 5.13 cm^2/V s. The enhanced mobility yielded by incorporating Al_2O_3 NPs potentially resulted because the nanocomposite layer is sufficiently robust to resist plasma damage during a-IGZO sputtering. The quality of the a-IGZO layer and the a-IGZO/gate dielectric interface are enhanced. To investigate its bending ability, the PEN substrate was manually roped on a ball pen with a tensile strain perpendicular to the channel for more than 100 times. Along this direction, the a-IGZO TFT is most likely to be damaged after bending.[11] The bending radius was 4 mm. The strain (σ) of the a-IGZO TFT on the PEN substrate (1.56%) was calculated by the following equation:

$$Strain(\sigma) = \frac{D}{2R}, \quad (1)$$

in which D is the total thickness (film and substrate) and the R is the bending radius. Fig. 4(a) shows the transfer characteristics of the a-IGZO TFT with either PVP or nanocomposite layer as dielectric exposed to various rope times. The transfer characteristics are only slightly altered after being fastened to the ball pen and released 100 times for a-IGZO TFT with nanocomposite layer. The IV curve shifted for a-IGZO TFT with polymer dielectric after bending. Figs. 4(b) and 4(c) show the extracted threshold voltage (V_{th}) and SS, respectively, for four a-IGZO TFTs comprise a nanocomposite dielectric. The V_{th} are slightly enhanced after 80 times of bending. This might be due to the re-distribution of nanoparticles after bending. The SS are kept in a small range for all devices after bending. As previously mentioned, this is due to material deformation, which primarily occurs on polymer nanocomposites under strain. This indicates the interface of a-IGZO/nanocomposite interface was almost unaltered. In contrast, the Vth and S.S. shifted clearly after bending. This could be explained by the chemistry property of PVP. The PVP was cross-linked by UV light illumination at low temperature. Some hydroxyl groups may exist in the polymer. These hydroxyl groups are unstable and containing charges. After bending, those charges may re-distribute. The re-distribution will cause the shift of the Vth and S.S. Table II compares the flexibility of this work to the references. Although the bending radius is not the smallest for this work, the strain is high at low process temperature. Thus, this robust a-IGZO TFT that employs nanocomposite polymer is suitable for use in flexible displays and electronics.

To evaluate the reliability, positive-gate-voltage stress at 8 V and 10 V was applied to a-IGZO TFT for 1500 s. Figures 5(a) and 5(b) depict the threshold voltage shift (ΔV_{th}) and S.S. of a-IGZO TFTs with and without Al_2O_3 NPs. Both TFTs with either polymer or nanocomposite gate dielectric exhibit negatively shifted ΔV_{th}. The ΔV_{th} as high

TABLE I. The electrical performance of a-IGZO TFTs.

Dielectric	μ (cm^2/V s)	S.S. (V/dec.)	I_{ON}/I_{OFF}	V_{th} (V)
Polymer	0.8	1.1	1.3×10^4	−1.4
0.25 wt. % Al_2O_3 NPs	5.13	0.84	1.4×10^5	2.3

TABLE II. Comparisons on the flexibility of a-IGZO TFT on plastic substrates for in this work and related.

Reference	Substrate	Process temperature (°C)	Substrate thickness (μm)	Bending radius (mm)	Strain (%)
3	PEN	150	125	N/A	N/A
5	Polyimide	350	10	3	0.17
6	Polyimide	115	50	2	1.25
7	Polyimide	N/A	25	2	0.63
This work	PEN	100	125	4	1.56

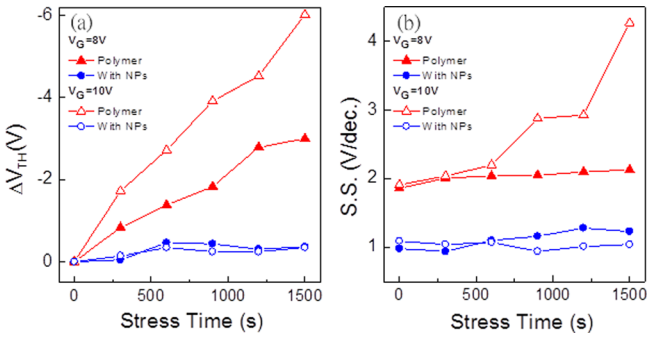

FIG. 5. The time dependence of the (a) ΔV_{th} and (b) S.S. extracted from I_D-V_G characteristics for a-IGZO TFT with gate dielectric uses either polymer of nanocomposite under positive-gate-bias stress ($V_G = 8$ and 10 V).

as −6 V was observed for the TFT with polymer gate dielectric after 1500 s stress. In contrast, ΔV_{th} as small as −0.34 V was found for a-IGZO TFT with nanocomposite gate dielectric. The S.S. for the TFT with polymer gate dielectric increased extensively from 1.8 to 4.3 V/dec. after 10 V positive gate voltage stress, whereas it is only increased from 0.98 to 1.23 V/dec. for TFT with nanocomposite gate dielectric. The negatively shifted threshold voltage and increased subthreshold swing are differed from general finding in the a-IGZO with inorganic dielectric.[12,13] In general, the threshold voltage will shift positively because of the electron trapping in the a-IGZO channel with less subthreshold swing changed. Therefore, the negatively shift V_{th}, must have additional mechanism other than electron trapping. The possible mechanism is the electron induced gate dielectric damage under high field. The high energy electron may break bonds of polymer that create positively charged states. These positive charges will cause V_{th} shift negatively. In addition to the gate dielectric, the a-IGZO/polymer interfaces also damaged. With Al_2O_3 nanoparticles incorporation, the damage was suppressed. As we mentioned above, the volume fraction of Al_2O_3 is estimated to 43%. This indicates most of PVP was surrounded by the robust Al_2O_3 NPs that alleviate the high energy carrier damage.

In summary, we have demonstrated high mobility a-IGZO TFT with polymer-nanoparticle composite gate dielectric on PEN. The mobility as high as 5.13 cm^2/V s was achieved. After rope the a-IGZO TFT for 100 times (4 mm radius, strain = 1.56%), the electrical characteristics are almost unchanged. With nanocomposite gate dielectric, the threshold voltage and subthreshold swing are less altered under positive gate voltage stress at 10 V after 1500 s. Such a-IGZO TFT has high potential as the addressing device in a flexible display.

This work was supported by Ministry of Science and Technology of Taiwan for financially under Grant NSC 102-2221-E-005-087.

[1]T. Kamiya and H. Hosono, NPG Asia Mater. **2**, 15 (2010).
[2]T. Arai and Y. Shiraishi, SID'12 Digst. **43**, 756 (2012).
[3]S. Yang, J. Y. Bak, S. M. Yoon, M. K. Ryu, H. Oh, C. S. Hwang, G. H. Kim, S. H. Park, and J. Jang, IEEE Electron Device Lett. **32**, 1692 (2011).
[4]H. Xu, D. Luo, M. Li, M. Xu, J. Zou, H. Tao, L. Lan, L. Wang, J. Penga, and Y. Cao, J. Mater. Chem. C **2**, 1255 (2014).
[5]J. S. Park, T. W. Kim, D. Stryakhilev, J. S. Lee, S. G. An, Y. S. Pyo, D. B. Lee, Y. G. Mo, D. U. Jin, and H. K. Chung, Appl. Phys. Lett. **95**, 013503 (2009).
[6]N. Münzenrieder, G. A. Salvatore, T. Kinkeldei, L. Petti, C. Zysset, L. Büthe, and G. Tröster, in *Proceedings of 71st Annual IEEE Device Research Conference (DRC)* (2013), p. 165.
[7]J. Jang, M. H. Choi, B. S. Kim, W. G. Lee, and M. J. Seok, "Robust TFT Backplane for Flexible AMOLED," SID'12 Digst. **43**, 260 (2012).
[8]A. Chida, K. Hatano, T. Inoue, N. Senda, T. Sakuishi, H. Ikeda, S. Seo, Y. Hirakata, S. Yamazaki, S. Yasumoto, M. Sato, Y. Yasuda, S. Okazaki, and W. Nakamura, "Seiichi Mitsui," SID'12 Digst. **44**, 196 (2013).
[9]H. C. Lai, B. J. Tzeng, Z. Pei, C. M. Chen, and C. J. Huang, SID'12 Digst. **43**, 764 (2012).
[10]Y. Zhou, S. T. Han, Z. X. Xu, X. B. Yang, H. P. Ng, L. B. Huang, and V. Roy, J. Mater. Chem. **22**, 14246 (2012).
[11]N. Münzenrieder, K. Cherenack, and G. Tröster, IEEE Trans. Electron Devices **58**, 2041 (2011).
[12]K. Hoshino, D. Hong, H. Q. Chiang, and J. F. Wager, IEEE Trans. Electron Devices **56**, 1365 (2009).
[13]M. D. H. Chowdhury, P. Migliorato, and J. Jang, Appl. Phys. Lett. **98**, 153511 (2011).